

## Evidences of Rare Earth Ion Aggregates in a Sol–Gel Silica Matrix: The Case of Cerium and Gadolinium

Daniela Di Martino,<sup>\*,†,‡</sup> Anna Vedda,<sup>†,‡</sup> Giuliano Angella,<sup>§</sup> Michele Catti,<sup>†,||</sup> Elena Cazzini,<sup>†</sup> Norberto Chiodini,<sup>†</sup> Franca Morazzoni,<sup>†,||</sup> Roberto Scotti,<sup>†,||</sup> and Giorgio Spinolo<sup>†,‡</sup>

*Dipartimento di Scienza dei Materiali, Università di Milano Bicocca, Milano, Italy, CNR, Istituto IENI, Sez. Milano Bicocca, Milano, Italy, INFN, CNR UdR Milano Bicocca, Milano, Italy, and INSTM, UdR Milano Bicocca, via Cozzi 53, I-20125 Milano, Italy*

Received May 8, 2004

Structural and morphological studies were carried out on cerium- and gadolinium-doped sol–gel silica glasses intended for scintillator applications, to deepen the understanding of rare earth ion incorporation into the glass matrix. Several compositions, ranging from 0 to 5 mol % Ce and from 0 to 8 mol % Gd, were studied by Raman spectroscopy. The vibrational response was compared to that of pure silica glasses: for cerium doping higher than 0.5 mol %, the  $F_{2g}$  Raman mode, characteristic of  $CeO_2$ , was observed. The presence of  $CeO_2$  nanocrystalline clusters, whose size depends on cerium concentration and thermal treatment, was confirmed also by X-ray powder diffraction (XRD) patterns and transmission electron microscopy (TEM) analyses. On the contrary, gadolinium-doped sol–gel silica glasses exhibited Raman spectra similar to those of pure silica glasses, at least for the investigated concentrations up to 8 mol %, and no crystalline particles were detected within the amorphous matrix.

### Introduction

Rare earth (RE) ions play key roles in many technological applications, mainly for their luminescence properties. The incorporation of RE ions into different amorphous matrixes has been largely investigated.<sup>1–3</sup> In particular, cerium is one of the most frequently considered activators in RE ion doped systems to be used as scintillator materials, due to the radiative transition (5d–4f, time decay lower than 100 ns) featured by trivalent cerium ions.<sup>4</sup> Recently, sol–gel-prepared Ce-doped silica glasses were shown to have excellent scintillator properties.<sup>5,6</sup> Various densification

processes of the xerogel were attempted to improve the glass optical properties,<sup>7,8</sup> and glasses were investigated in detail. In parallel to optical studies, structural and morphological investigation appeared to be useful, and the present work is specifically aimed at shedding further light on the incorporation of Ce ions into the sol–gel silica matrix. Considering that two different oxidation states,  $Ce^{3+}$  and  $Ce^{4+}$ , are possible, the highest quantity of  $Ce^{3+}$  is desirable,  $Ce^{4+}$  being not luminescent. As a matter of fact, an important requirement in obtaining  $Ce^{3+}$ -doped glasses by the classical melting/quenching technique is the use of reducing atmosphere during melting.<sup>9</sup> Nevertheless, loss of the luminescence yield may be due to thermodynamics limitations, i.e., insufficient solubility of the RE, with the consequent separation of microphases and concentration quenching.<sup>10</sup> This effect occurs at high doping levels, when RE ion distance becomes comparable to the critical radius, that is, the distance at which the radiative decay probability equals the energy transfer rate, finally leading to nonradiative processes.<sup>4</sup> Obviously, the above-mentioned peculiarities are not the only ones affecting luminescence, since other nonradiative channels can be active. The most frequent ones are related to the presence of OH groups and other defect species. Con-

\* Corresponding author. Phone: +39-02-64485162. Fax: +39-02-64485400. E-mail: daniela.dimartino@mater.unimib.it.

<sup>†</sup> Università di Milano Bicocca.

<sup>‡</sup> INFN.

<sup>§</sup> CNR.

<sup>||</sup> INSTM.

(1) Reisfeld, R.; Jorgensen, C. K. *Optical properties of colorants or luminescent species in sol–gel glasses, Structure and Bonding*; Reisfeld, R., Jorgensen, C. K., Eds.; Springer-Verlag: 1992; Vol. 77, p 207.

(2) Rodnyi, P. A. *Physical processes in inorganic scintillators*; CRC: Boca Raton, FL, 1997.

(3) Many of the rare earth properties and applications can be found in the *Proceedings of the International Conference on Inorganic Scintillators and Their Use in Scientific and Industrial Applications*. See, for example, the proceeding of SCINT 2001 (Chamonix, France): *Nucl. Instrum. Methods Phys. Res.* **2002**, *A486*.

(4) Blasse, G.; Grabmaier, B. C. *Luminescent materials*; Springer-Verlag: Berlin, 1994.

(5) Chiodini, N.; Fasoli, M.; Martini, M.; Rosetta, E.; Spinolo, G.; Vedda, A.; Nikl, M.; Solovieva, N.; Baraldi, A.; Capelletti, R. *Appl. Phys. Lett.* **2002**, *81*, 4374.

(6) Chiodini, N.; Vedda, A.; Baraldi, A.; Martini, M.; Nikl, M.; Scotti, R.; Spinolo, G. High efficiency luminescent glasses, particularly for use as scintillating materials for the detection of ionizing radiation, and corresponding production process. Italian Patent, 2001, MI2001 A002555, and PCT International Patent Application, 2002, PCT/IT02/00756.

(7) Vedda, A.; Baraldi, A.; Canevali, C.; Capelletti, R.; Chiodini, N.; Francini, R.; Martini, M.; Morazzoni, F.; Nikl, M.; Scotti, R.; Spinolo, G. *Nucl. Instrum. Methods Phys. Res.* **2002**, *A486*, 259.

(8) Chiodini, N.; Fasoli, M.; Martini, M.; Morazzoni, F.; Rosetta, E.; Scotti, R.; Spinolo, G.; Vedda, A.; Nikl, M.; Solovieva, N.; Baraldi, A.; Capelletti, R.; Francini, R. *Radiat. Effects Defects Solids* **2003**, *158*, 463.

(9) Spowart, A. R. *Nucl. Instrum. Methods* **1976**, *135*, 441.

(10) Auzel, F.; Goldner, P. *Opt. Mater.* **2001**, *16*, 93.

cerning the detection of OH groups, their presence in glasses was investigated by IR absorption.<sup>11,12</sup>

The complete comprehension of the luminescence features of Ce (as well as other RE ions) in the silica matrix requires extended fundamental investigation taking into account several aspects of the material. Therefore, in the following, focusing our interest on a structural and morphological study, the results of the characterization of Ce-doped sol-gel silica glasses by Raman spectroscopy, X-ray diffraction (XRD), and transmission electron microscopy (TEM) are reported. Moreover, a comparison is made with the Raman features of Gd-doped sol-gel silica glasses where the RE is in the very stable trivalent oxidation state. Such comparison mainly discloses a different tendency in clustering between Ce and Gd ions. In fact, for cerium doping higher than 0.5 mol %, CeO<sub>2</sub> crystals with a size distribution in the range 5–20 nm were observed, while no evidence of the presence of Gd<sub>2</sub>O<sub>3</sub> crystals was obtained at least up to 8 mol % Gd.

### Experimental Section

**Preparation of Glasses.** Silica glasses with a molar percentage [mol % = moles of RE/(moles of RE + moles of Si) × 100%] in the range 0–5.0 for Ce and 0–8.0 for Gd were prepared by the sol-gel method.

Tetraethyl orthosilicate (TEOS, Aldrich, 99.999%), Ce(NO<sub>3</sub>)<sub>3</sub>·6H<sub>2</sub>O (Aldrich, 99.99%), and Gd(NO<sub>3</sub>)<sub>3</sub>·6H<sub>2</sub>O (Aldrich, 99.99%) were used as precursors.

TEOS (2.0 mL) was mixed with ethanol (HPLC grade reagent) and with suitable amounts of Ce(NO<sub>3</sub>)<sub>3</sub>·6H<sub>2</sub>O or Gd(NO<sub>3</sub>)<sub>3</sub>·6H<sub>2</sub>O in about 0.1 M ethanol solutions, according to the glass composition. The volume of pure ethanol depended on the amount of RE solution, as the total volume solution was 8.0 mL.

Finally, 1.20 mL of water (Merck analytical grade) was added with stirring (H<sub>2</sub>O:TEOS molar ratio 7.4).

The resulting clear solutions were sealed in polypropylene containers (5 cm in diameter) and stored in a thermostatic chamber at 35 °C. Gelation occurred in 10–20 days. Afterward, samples were aged for 2 days and, subsequently, small holes were produced in the container covers in order to induce slow drying of the alcogel. Drying of the alcogels was reached in about 1–2 weeks at 35 °C, yielding transparent xerogels.

Densification of xerogels to glasses was carried out through a sintering procedure up to 1050 °C, which alternated oxygen and reduced pressure steps. Specifically, samples were heated under an oxygen stream up to 450 °C (heating rate 6 °C/h) and maintained at this temperature for 24 h, and then samples were more slowly heated to 1050 °C (4 °C/h) under reduced pressure (1.33 Pa) or inert atmosphere. However, we remark that the use of these two different atmospheres in the final densification stage did not significantly influence the investigated properties of the materials. Finally, the oven was switched off and the temperature decreased to room temperature in about 10 h.

Plates 15 mm in diameter and 1 mm thick (sometimes in fragments) were obtained. Microprobe XRF analyses, performed on Ce-doped silica glasses, confirmed the nominal compositions of cerium. Besides, OH content, monitored by IR absorption, was lower than 1 mol %.<sup>11,12</sup> A rapid thermal treatment (RTT) was performed after densification at 1050 °C on some samples, by using an oxidizing oxygen-hydrogen flame: after a very quick temperature increase (2–4 s), the sample was kept at 1800 ± 50 °C for approximately 10 s and

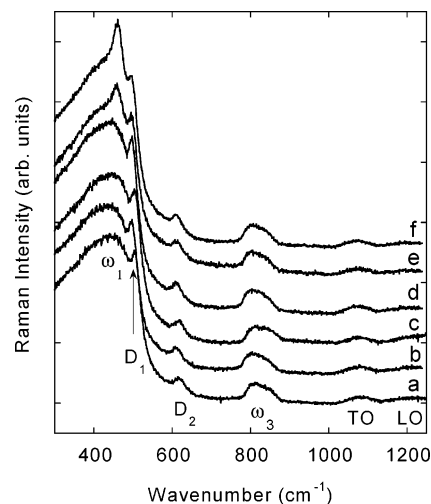


**Figure 1.** Raman spectra collected on gadolinium- and cerium-doped sol-gel silica glasses. The spectra are shifted on the ordinate scale for better clarity, and the letters refer to composition (a = undoped, b = 0.1 mol % Gd, c = 3 mol % Gd, d = 0.05 mol % Ce, e = 0.1 mol % Ce, f = 1 mol % Ce). The labels refer to the vibration assignments, made according to the literature.<sup>13,14</sup>

then rapidly cooled in air. The temperature was monitored by an optical pyrometer (Impac IE 120) working at 5.14 μm emission. The positive effect of this treatment on the RL of the present glasses was recently outlined.<sup>5</sup>

**Apparatus and Measurements.** Raman spectra were recorded at room temperature, by a micro-Raman spectrometer (Labram, Jobin-Yvon), equipped with a microscope. The excitation source was an internal He-Ne laser (632.8 nm), and the unpolarized Raman spectra were collected in backscattering configuration through a CCD (charge coupled device) detector. A commercial powder of crystalline CeO<sub>2</sub> (Aldrich, 99.99%) was used as a reference sample.

XRD measurements were carried out by a Bruker D8 Advance spectrometer (Cu Kα radiation) in the 5°–70° 2θ range, with step time from 5 to 8 s for a 0.02° Δ(2θ) step.

TEM analyses were carried out on 1 mol % Ce doped powdered silica glasses before (sample a) and after RTT (sample b). The original silica samples were ground into an agate mortar, and the resulting fine powder was put in distilled water. A drop of such a slurry was deposited on a carbon film supported on a 3 mm copper grid for TEM observations. After drying, TEM observations were performed using a JEOL 2000CX FII at 150 kV. Microdiffraction patterns from particles found in sample b were obtained by finely converging the electron beam in such a way that the illuminated area was smaller than the particle size (about 20 nm).

### Results and Discussion

Raman spectra were obtained on cerium- and gadolinium-doped silica glasses at various dopant concentrations. Typical spectra are reported in Figure 1, the general features resembling those corresponding to pure silica glass. Three bands and two peaks are clearly visible: the band at ~440 cm<sup>-1</sup> (labeled ω<sub>1</sub>) corresponds to the Si-O symmetric stretching vibration,<sup>13</sup> while the two peaks at 490 and 603 cm<sup>-1</sup> (labeled respectively D<sub>1</sub> and D<sub>2</sub>) are related to the stretching vibrations of planar tetrahedra rings of 4- and 3SiO<sub>4</sub>.<sup>14</sup> In addition, the band at ~800 cm<sup>-1</sup> (labeled ω<sub>3</sub>) is related to the mixed

(11) Baraldi, A.; Capelletti, R.; Chiodini, N.; Mora, C.; Scotti, R.; Uccellini, E.; Vedda, A. *Nucl. Instrum. Methods Phys. Res.* **2002**, *A486*, 408.

(12) Baraldi, A.; Capelletti, R.; Chiodini, N.; Oppici, C.; Scotti, R.; Vedda, A. *Radiat. Effects Defects Solids* **2003**, *157*, 1139.

(13) Galeener, F. L.; Geissberger, A. E. *Phys. Rev.* **1983**, *B27*, 6199.

(14) Galeener, F. L. *Solid State Commun.* **1982**, *44*, 1037.

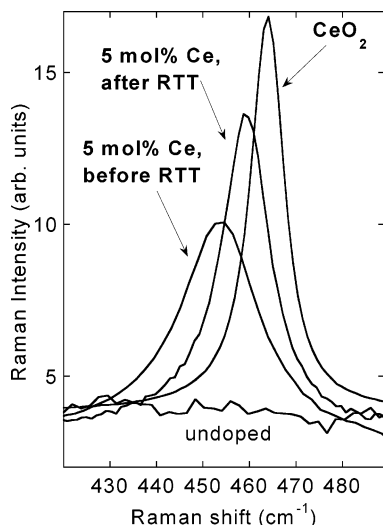


**Figure 2.** Raman spectra obtained on three different samples (pure raw powder of  $\text{CeO}_2$  and 5 mol % Ce doped sol-gel silica glass before and after RTT) compared with an undoped sol-gel silica glass.

stretching-bending Si-O vibration, while the structures at around 1070 and 1200  $\text{cm}^{-1}$  are due to transverse optical (TO) and longitudinal optical (LO) Si-O stretching.<sup>13</sup> In the case of gadolinium-doped glasses, no change in the vibrational response was revealed. In fact, after background subtraction and normalization to the  $\omega_3$  silica band at  $\sim 800 \text{ cm}^{-1}$ , all Raman spectra can be easily superimposed, and they resemble the Raman spectra of pure silica glass. The same behavior occurs at low cerium concentrations (in the range 0–0.1 mol %). On the contrary, in the range 0.5–5 mol % Ce, the appearance of a Raman peak at  $\sim 460 \text{ cm}^{-1}$  was evident. This peak could be assigned to a  $\text{CeO}_2$  crystalline phase, after comparison with a commercial powder of pure  $\text{CeO}_2$ , yielding a symmetrical stretching vibration ( $F_{2g}$  symmetry of a fluorite structure) at  $464 \text{ cm}^{-1}$ .<sup>15</sup> The Raman spectra obtained on different samples (undoped glass, 5 mol % Ce doped glass before and after RTT, and  $\text{CeO}_2$  crystalline powder) in the wavenumber interval 420–490  $\text{cm}^{-1}$  are shown in Figure 2. A difference among the spectra, both in the peak positions and in the full width at half-maximum (FWHM) of the Raman peak is evident. Figure 3a,b reports the behavior of the peak position and the FWHM for all the investigated samples, the positions and FWHM being obtained by a Lorentian peak fitting after background subtraction and peak normalization to a sol-gel-prepared pure silica Raman spectrum. A very likely origin of this behavior may be the different  $\text{CeO}_2$  crystalline size. The vibrational response of  $\text{CeO}_2$  nanocrystals in ceria and/or other systems was already disclosed in the literature<sup>16–18</sup> assessing that nanocrystalline sizes induce (i) a shift of the peak position, moving toward lower wavenumbers by decreasing the nanocrystalline size, as well as (ii) a widening of the Raman bands, the wider the size of

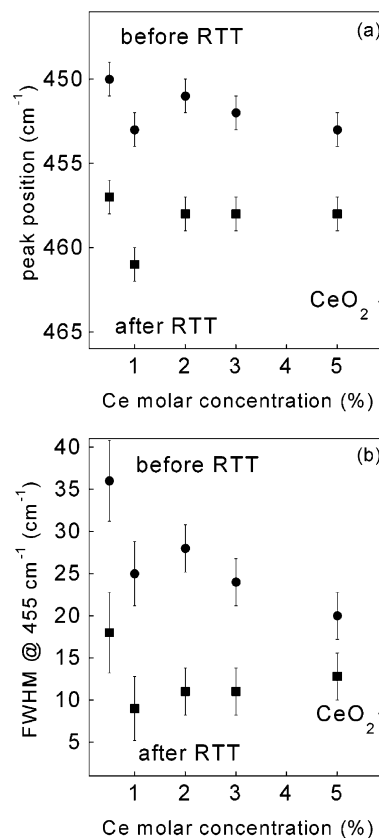


**Figure 3.** Behavior of (a) Raman peak position and (b) FWHM as a function of the Ce content and thermal treatment (before and after RTT). As a comparison, the last datum (up-triangle) corresponds to pure crystalline  $\text{CeO}_2$ . All data were derived by Lorentzian peak fitting of the symmetric stretching vibration ( $F_{2g}$ ) relative to  $\text{CeO}_2$  structure.

the nanocrystals the more peaked and symmetric the Raman vibration. As a matter of fact, it was not possible to explain by a single model both the change in the Raman shift and the widening of the peaks by varying the crystalline size.<sup>16–18</sup> Nevertheless, the widening of the Raman feature for a crystalline size in the nanometer range—observed also in silicon nanocrystalline systems—is a consequence of the contribution of both bulk and surface transverse and longitudinal optical modes.<sup>19</sup> Moreover, in the case of cerium oxide nanocrystals, TEM evidence was presented of lattice relaxation and expansion, accounting for the shift of the Raman peak position.<sup>20</sup> In glasses treated by RTT, the Raman peak position due to Ce-O vibration shifts to higher wavenumbers (Figures 2 and 3), and the width of the Raman peak decreases with respect to the corresponding glasses before RTT, indicating that the initial size of the  $\text{CeO}_2$  nanocrystals gets larger after RTT.

XRD patterns gave direct evidence of  $\text{CeO}_2$  nanocrystals in RTT glasses, whereas no diffraction peaks could be detected in non-RTT samples with less than 5 mol % Ce (cf. the 1% case in Figure 4). Raman spectra cannot give directly the value of the  $\text{CeO}_2$  cluster dimensions, but need calibration through XRD or TEM

(15) Weber, W. H.; Hass, K. C.; McBride, J. R. *Phys. Rev.* **1993**, *B48*, 178.

(16) Spanier, J. E.; Robinson, R. D.; Zhang, F.; Chan, S. W.; Herman, I. P. *Phys. Rev.* **2001**, *B64*, 245407.

(17) Zhang, F.; Chan, S.; Spanier, J. E.; Apak, E.; Jin, Q.; Robinson, R. D.; Herman, I. P. *Appl. Phys. Lett.* **2002**, *80*, 127.

(18) Kosacki, I.; Suzuki, T.; Anderson, H. U.; Colomban, P. *Solid State Ionics* **2002**, *149*, 99.

(19) Iqbal, Z.; Vepřek, S. *Journal of Physics C: Solid State Physics* **1982**, *15*, 377.

(20) Tsunekawa, S.; Ishikawa, K.; Li, Z.-Q.; Kawazoe, Y.; Kasuya, A. *Phys. Rev. Lett.* **2000**, *85*, 3440.

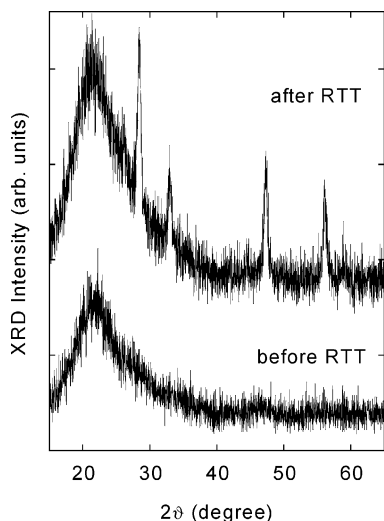


**Figure 4.** XRD patterns collected on 1 mol % Ce glass before and after RTT.

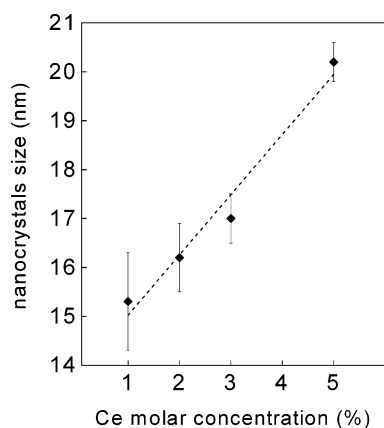


**Figure 5.** Size of  $\text{CeO}_2$  nanocrystals in the silica matrix (after RTT) plotted against the Ce content, from XRD data. The full-widths at half-height of the X-ray Bragg peaks were analyzed with the Scherrer equation.

analysis. By use of the full widths at half-height of the  $\text{CeO}_2$  X-ray diffraction peaks, analyzed through the Scherrer equation, the mean crystalline size was determined in the glasses containing 1, 2, 3, and 5 mol % Ce after RTT, obtaining values in the 15–20 nm range (Figure 5). A calibration on well-crystallized  $\text{CeO}_2$  was taken into account. The error bars in Figure 5 correspond to deviations between results from different Bragg peaks in the  $\text{CeO}_2$  XRD pattern. In the case of the 5% sample before RTT, very broad peaks appeared corresponding to a crystal size of about 5 nm.

Also TEM measurements confirmed the existence of  $\text{CeO}_2$  particles in the 1 mol % Ce doped silica glasses, both before and after RTT (see Figure 6). Moreover, the mean size of  $17 \pm 2$  nm was evaluated over 100-particle analysis in the 1 mol % Ce doped silica glass after RTT, and microdiffraction gave the pattern of  $\text{CeO}_2$  displayed in Figure 7. In fact, the pattern is from a face-centered cube crystallographic structure with a calculated rectangular parameter of 0.546 nm.

Concerning Gd-doped glasses, no peak was disclosed in the XRD patterns, thus supporting the absence of any crystalline particle segregation. Moreover, the Raman spectrum of  $\text{Gd}_2\text{O}_3$  raw powder shows a peak at  $360 \text{ cm}^{-1}$ . The absence of this peak in the Raman spectra of

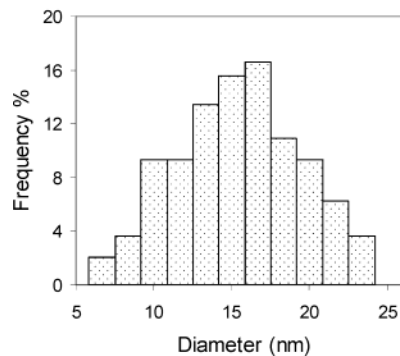
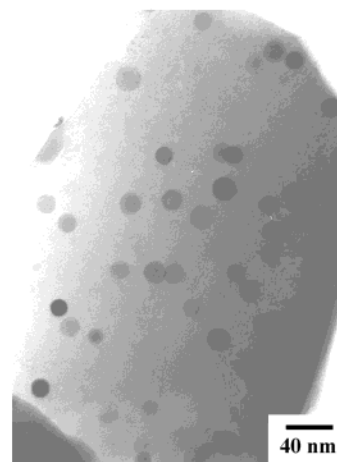
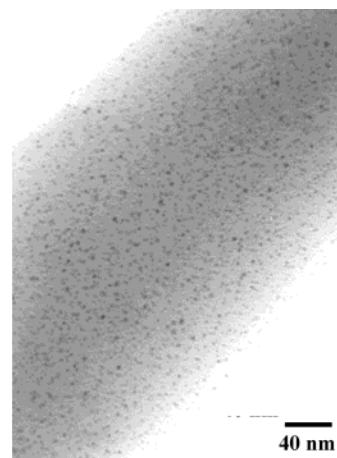


**Figure 6.** TEM images of 1 mol % Ce doped glass before (upper picture) and after RTT (lower picture). In the bottom of part b the statistical distribution of the size of  $\text{CeO}_2$  nanocrystals is shown over 100 clusters analysis.

Gd-doped glasses can be accounted for by the absence of any  $\text{Gd}_2\text{O}_3$  crystalline particle within the amorphous matrix (at least with dimensions higher than  $\sim 10$  nm). Accordingly, the absence of Gd-clustering effects inside different glasses is reported in many papers in the literature,<sup>21</sup> which support only an incipient phase ordering, immiscibility, and heterogeneity in the amorphous state but not the presence of Gd aggregates.

The here described phenomenology really demonstrates  $\text{CeO}_2$  aggregate formation with Ce ions in the +4 oxidation state in our glasses, thus indicating the attitude of  $\text{Ce}^{3+}$  to be oxidized, under the conditions here

(21) Zhang, Y.; Navrotsky, A.; Li, H.; Li, L.; Davis, L. L.; Strachan, D. M. *J. Non-Cryst. Solids* **2001**, *296*, 93 (and refs 17, 21–24 therein).

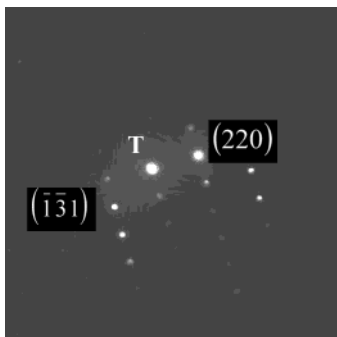


**Figure 7.** Microdiffraction patterns collected on 1 mol % Ce doped silica glass after RTT. Results are in agreement with literature  $\text{CeO}_2$  data.

reported for the preparation of glasses. It could appear difficult to give a rationale for the  $\text{Ce}^{3+}$  oxidation, given the high potential of the  $\text{Ce}^{3+}/\text{Ce}^{4+}$  in aqueous acid solution (from 1.44 V in 1 M  $\text{H}_2\text{SO}_4$  to 1.70 V in 1 M  $\text{HClO}_4$ ).<sup>22</sup> However, considering that cerium ions are surrounded by hydroxo-oxo groups, deriving from water and alcohol complexation in the gel phase, we expect

(22) Greenwood, N. N.; Earnshaw, A. In *Chemistry of the Elements*; Pergamon Press Ltd.: New York, 1985; p 1444.

that complexation and hydrolysis may lower the potential and finally give, like in alkaline solution, the precipitation of  $\text{CeO}_2$ .<sup>22</sup>

### Conclusion

Raman spectra, XRD, and TEM measurements were collected for several cerium- and gadolinium-doped sol-gel silica glasses. Main results assess that these two RE ions have a different behavior upon insertion in a sol-gel silica matrix, resulting in a favorable RE oxide segregation in the case of cerium.

$\text{CeO}_2$  aggregates were indeed disclosed within the amorphous matrix, bigger  $\text{CeO}_2$  clusters being unveiled in the glasses after RTT. This structural and morphological evidence could be of interest in the search for the highest yield luminescent material.

**Acknowledgment.** This work is part of national projects (PRIN2001 and PRIN2002) supported by the Italian Ministry of University Research and Technology. The authors gratefully thank Dr. J. Mares of the Institute of Physics, Academy of Science, Prague, for XRF measurements.

CM049276M